

# CLAD-Net: Continual Activity Recognition in Multi-Sensor Wearable Systems

Reza Rahimi Azghan\*, Gautham Krishna Gudur†, Mohit Malu\*  
 Edison Thomaz†, Giulia Pedrielli\*, Pavan Turaga\*, Hassan Ghasemzadeh\*

**Abstract**—The rise of deep learning has significantly advanced human behavior monitoring using wearable sensor data. In particular, human activity recognition (HAR) through deep models has been extensively explored. However, most existing methods assume a stationary data distribution, an assumption that often breaks down in real-world settings. For instance, sensor data collected from one subject performing an activity may differ substantially in distribution from that of another subject. In continual learning settings, this shift is modeled as a sequence of tasks—where each task corresponds to a new subject—which makes the system susceptible to catastrophic forgetting, where previously learned patterns degrade as new ones are acquired. This challenge is further exacerbated by the reliance on labeled data, which is often sparse or inconsistently available in studies involving human participants. To address these challenges, drawing inspiration from complementary learning systems, we introduce CLAD-Net—Continual Learning with Attention and Distillation—an innovative framework that enables deep models in wearable sensor systems to be updated continuously without compromising performance on previously learned tasks. CLAD-Net combines a self-supervised transformer, serving as the system’s long-term memory, with a supervised Convolutional Neural Network (CNN) trained with knowledge distillation for activity classification. The transformer captures global activity patterns through cross-attention across body-mounted sensors and learns generalizable representations without requiring labels. In parallel, the CNN incorporates knowledge distillation to retain past knowledge during subject-wise fine-tuning. We evaluate CLAD-Net under a continual stream of data from multiple subjects and show that it achieves 91.36% final accuracy with only 8.78% forgetting on the PAMAP2 dataset, outperforming well-established memory-based and regularization-based methods such as Experience Replay and Elastic Weight Consolidation. Furthermore, in semi-supervised settings with only 10–20% labeled data, CLAD-Net maintains superior performance, showcasing its robustness to label scarcity. Extensive ablation studies also confirm the contribution of each module to the system’s overall effectiveness.

**Index Terms**—Human Activity Recognition, Continual Learning, Catastrophic Forgetting, Attention Models, Self-Supervised Learning

## I. INTRODUCTION

Adapting to dynamic environments is a fundamental characteristic of any intelligent system. Through years of evolution, humans have developed the ability to adjust to new situations without losing previously acquired knowledge. Ideally, AI systems should exhibit a similar capability—acquiring tasks sequentially while performing as if all tasks were learned simultaneously. Despite their remarkable capacity to learn

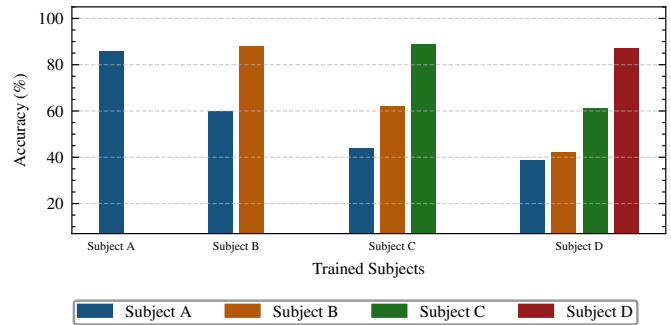


Fig. 1. Fine-tuning the model on new subjects leads to a decline in accuracy on previously seen subjects

from data streams, many systems still struggle with retaining past knowledge [1], [2]. Learning continually from data allows models to balance the stability-plasticity trade-off [3], which in turn enables them to generalize to future tasks while preserving prior learning. However, in practice, models often prioritize plasticity over stability. This leads to a phenomenon known as catastrophic forgetting. The issue becomes even more severe when the new tasks differ significantly in distribution from previous ones [4].

A major challenge for machine learning systems deployed in real-world settings is the continuous exposure to distribution shifts in the data stream [5], [6]. Unlike in controlled environments, training data in such contexts no longer follows an i.i.d. process [7]. Instead, there is often an inherent shift in the distribution of incoming data points over time [5]. For example, in human activity recognition (HAR), a model trained on data from one subject may struggle when applied to a new subject, as individuals often perform the same activities in distinct ways [8], [9]. This can result in the model either failing to generalize to the new subject or forgetting the learned decision boundaries for previous ones. A simple illustration of this issue is presented in Fig. 1, where a 7-layer MLP is trained on the first four subjects of the PAMAP2 dataset [10]. As the model is sequentially trained on new subjects, its accuracy on earlier ones steadily declines.

Additionally, most intelligent systems operate under the assumption that abundant labeled data is available for training. However, in real-world applications, this assumption is often unrealistic [11]–[13]. Labeling is typically the responsibility of subjects themselves, who may not consistently follow the data collection protocol. In activity recognition tasks using sensor data, for instance, participants might forget to label the actions

\*Arizona State University, Phoenix, AZ, USA,

† The University of Texas at Austin, Austin, TX, USA

they perform, further complicating the downstream learning process.

To tackle these challenges, many research directions draw inspiration from how humans learn and retain knowledge [14]. For example, the human mind often revisits past experiences to reinforce memory, an idea reflected in Experience Replay (ER) [15]–[17]. Additionally, humans naturally retain prior knowledge while learning new skills. The brain preserves learned representations even as it acquires new information, much like distillation-based methods [18]–[20], which helps neural networks retain responses to earlier tasks during adaptation to new ones. Furthermore, the brain employs distinct mechanisms for long-term and short-term memory, using complementary systems [21], [22] to encode new experiences while preserving past knowledge—a principle echoed in models like DualNet [22] and Kaizen. [23].

Humans also excel at learning from unstructured, unlabeled data. Infants, for instance, recognize objects and speech patterns by predicting and associating outcomes from raw sensory input [24]–[26]. This ability to derive learning signals from context aligns with self-supervised learning, where models extract useful representations through pretext tasks without labeled data [12]. Although many self-supervised methods have been developed to address label scarcity, their role in improving knowledge retention for downstream classifiers remains an open question [27].

In this work, we focus on mitigating catastrophic forgetting in HAR using IMU sensor data collected from various body locations. Our approach, CLAD-Net, draws on the principles of knowledge distillation and complementary learning systems. Specifically, we employ two parallel models: one learns general patterns across the data—irrespective of activity type or subject—by leveraging cross-attention mechanisms in transformers and self-supervised training. We argue that this abstraction helps retain prior knowledge more effectively. The second model focuses on extracting discriminative features for activity classification. Outputs from both models are then combined and fed into a simple classification head to make final predictions.

In summary, the novelties of this work can be summarized as follows:

- We tackle the problem of domain-incremental learning in the context of HAR. The model is exposed to time-series data from new subjects over time and is required to generalize to their activities while retaining knowledge of activities from previously seen subjects.
- We introduce a two-component architecture designed to reduce forgetting. The backbone of CLAD-Net is a transformer that incorporates cross-attention across sensor readings from different body parts and is trained using a self-supervised learning framework. The CNN part of CLAD-Net is trained using a knowledge distillation approach. This combination addresses both the challenges of catastrophic forgetting and limited label availability.
- We conduct extensive experiments on two benchmark activity recognition datasets, demonstrating that CLAD-Net outperforms several state-of-the-art methods. Additional ablation studies further highlight the effectiveness of the

attention mechanisms and the model’s robustness under label-scarce conditions.

## II. RELATED WORK

HAR using wearable sensors has long been a central task in sensor-based applications. It involves detecting and classifying physical activities such as walking, standing, running, or cycling, based on time-series data collected from subjects and their environment, often through inertial sensors like accelerometers and gyroscopes. In recent years, deep learning approaches, particularly convolutional neural networks (CNNs), have shown strong performance in extracting discriminative features from such sensor data [9], [28]–[30]. However, these models face significant challenges in real-world deployments [31]. They are prone to catastrophic forgetting when exposed to new subjects or data distributions, a limitation that has led to growing interest in continual learning for HAR [9], [32], [33]. Furthermore, these systems often rely heavily on labeled data, which may be limited or inconsistently available in human studies. To mitigate this, recent self-supervised approaches like those proposed by [11], [12], [34] have demonstrated the value of large-scale pretraining on unlabeled sensor data to improve robustness and generalization. Despite these advances, effectively addressing both forgetting and label scarcity in HAR remains an open and important problem [22], [27].

Continual learning, which aims to overcome the problem of catastrophic forgetting, has traditionally been studied somewhat separately from HAR. It focuses on training models under non-stationary data distributions, where new tasks are presented sequentially over time [3], [35]. This paradigm is often referred to as lifelong learning or incremental learning in the literature, with the terms being used interchangeably in most cases [1], [36]. The core goal is to enable models to adapt to new tasks or data domains without forgetting previously learned knowledge—a capability essential for real-world HAR systems that operate over extended periods or across diverse users. Continual learning research is typically categorized into three main scenarios [4], [37]:

- Domain-incremental learning: Tasks share the same label space but differ in data distribution—for example, recognizing the same activities across different users or sensor setups.
- Task-incremental learning: Each task has a distinct label space and distribution, and task identities are provided during both training and evaluation.
- Class-incremental learning: Like task-incremental learning, but task identities are only available during training.

Many continual learning approaches are inspired by how the human brain handles forgetting. Methods such as [38] and [39] follow the idea of complementary learning systems, separating short-term and long-term memory components within the architecture. In contrast, simpler strategies like ER using memory replay, where a small memory buffer stores samples from previous tasks to help the model retain past knowledge during training on new data [15]. Other approaches, like [40] and [20], adopt knowledge distillation, penalizing the

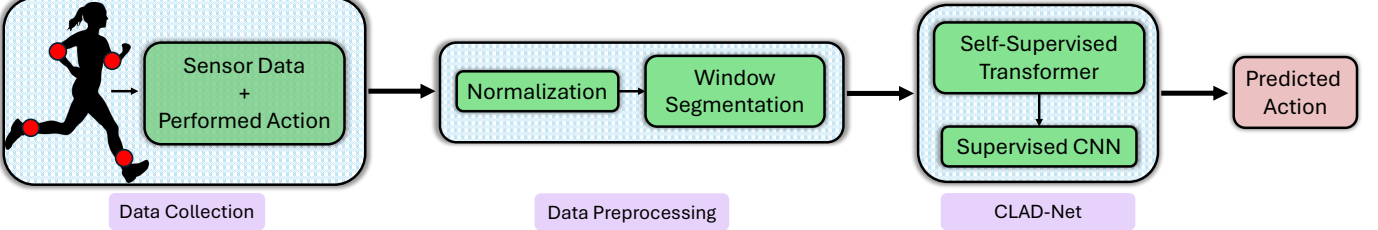


Fig. 2. The complete pipeline of the proposed system, composed of three core components: data collection, data preprocessing, and the final model, CLAD-Net.

model when its parameters deviate significantly while learning new tasks. While much of the existing research has focused on image data, interest in continual learning for time-series data—especially in HAR—has grown in recent years. [32] evaluated a range of continual learning approaches, including both regularization-based techniques and rehearsal methods, on several HAR time-series datasets. In another study, [41] proposed an attentive recurrent neural network to combat catastrophic forgetting in HAR, showing that incorporating attention mechanisms into lightweight models can effectively support continual learning.

Transformers have recently emerged as powerful models for sensor-based HAR, largely inspired by the success of Vision Transformers (ViTs) in computer vision, which model spatial relationships by treating image patches as sequences [42]–[44]. In wearable HAR, a similar principle applies—sensor readings over time or across body locations can be treated as sequences or segments for attention-based modeling. A core innovation in this domain is the use of cross-attention mechanisms to capture dependencies between distinct body parts, sensor modalities, or temporal patterns. For instance, [45] proposed a cross-attention enhanced pyramid network that establishes interrelationships across sensor channels, time steps, and feature dimensions, enabling the model to suppress noise and amplify activity-relevant signals. Similarly, [46] introduced a triple-attention framework that performs attention across sensor, temporal, and channel axes, showing that cross-dimensional fusion yields significant improvements in HAR performance. [47] took a top-down approach by proposing a “reverse attention” mechanism, where global contextual features attend back to individual sensor streams. [48] presented a two-stream transformer architecture that separately models temporal dynamics and cross-sensor spatial relationships, fusing them through attention-weighted integration to account for both intra-sensor sequences and inter-sensor configurations. Collectively, these models demonstrate the growing role of cross-attention in HAR and offer a principled way to model complex spatial-temporal patterns across the human body using wearable sensor data.

### III. PROPOSED APPROACH

#### A. System overview

In this section, we describe the components of our proposed system, following the overall flow from data sensing to model

transfer and evaluation. As illustrated in Fig. 2, the system is composed of three main components.

The first component is the data collection module, where inertial sensors are installed on various parts of the subject’s body as they perform a predefined set of activities. Subjects are also asked to provide the system with activity labels to indicate the type of activity they were performing at any given instant.

The second component is the data fetching and preprocessing module. Here, the raw sensor data collected from each subject is aggregated and normalized on a per-subject basis. A window segmentation algorithm is then applied to divide the continuous sensor streams into fixed-length segments. Each window is assigned a label if the corresponding activity is provided by the subject. Formally, each labeled window can be represented as  $(\mathbf{x}, y)$ , where  $\mathbf{x} \in \mathbb{R}^{l \times d}$ , with  $l$  being the window length and  $d$  the number of sensor channels. Since our experiments include a semi-supervised learning setup, labels  $y$  may not be available for every window.

The third and final component is the proposed machine learning model, which is designed to classify input windows into their corresponding activity labels. The main goal of the model is to maintain high classification accuracy for each new subject while minimizing the loss of information about previously seen subjects. To this end, we introduce a two-part architecture optimized with distinct objective functions, which are described in the following subsections .

#### B. Theoretical Background

In this work, we formulate the problem of continual learning in the application of human activity recognition as a domain-incremental learning paradigm. At each task  $t \in \{1, \dots, T\}$ , the system receives a batch of input-label pairs  $\mathcal{D}_t = \{(\mathbf{x}_{i,t}, y_{i,t})\}_{i=1}^{N_t}$ , where  $\mathbf{x}_{i,t} \in \mathbb{R}^{L \times d}$  denotes a multivariate time-series of length  $L$  with  $d$  sensor channels (e.g., accelerometer, gyroscope), and  $y_{i,t} \in \mathcal{Y}$  is the corresponding activity label.  $T$  is the number of overall subjects, and each task  $t$  corresponds to a distinct subject associated with a domain-specific distribution  $\mathcal{D}_t \sim \mathbf{P}_t(\mathbf{x}, y)$ .

Under the domain-incremental learning setting, we assume a static label distribution across tasks, i.e.,

$$\mathbf{P}_t(y) = \mathbf{P}_{t+1}(y), \quad \forall t \in \{1, \dots, T-1\}$$

but allow the marginal distribution over the time-series data to vary, such that

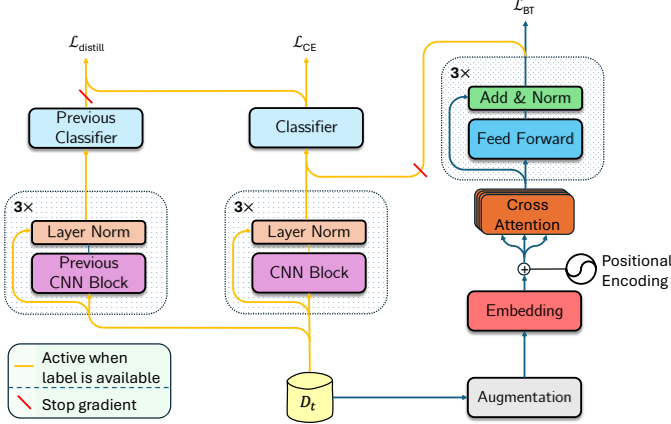


Fig. 3. Overview of CLAD-Net, including its architectural components and training workflow.

$$\mathbf{P}_t(\mathbf{x}) \neq \mathbf{P}_{t'}(\mathbf{x}), \quad \forall t \neq t'$$

Like in real settings, CLAD-Net is exposed to a continuum of the data points  $\{(\mathbf{x}_{i,t}, y_{i,t}, t)\}$ , where the distribution can be changed from  $\mathbf{P}_t$  to  $\mathbf{P}_{t+1}$  at any instant. Also, to reflect the constraints of real-world, memory-bound systems, the model does not have access to data from previous domains.

### C. CLAD-Net

CLAD-Net is composed of two key modules, as illustrated in Fig. 2. The first is a self-supervised transformer that functions as the architecture's long-term memory. This component operates independently of the task (subject) identifier and activity label, and only relies on dynamically distributed input variables.

The second module is a CNN-based classifier that processes the raw time-series data along with their corresponding labels. During training and inference, the representation learned by the transformer is concatenated with the classifier's final feature layer. This knowledge consolidation allows the classifier to benefit from the transformer's long-term representations. Further details on the architecture of both modules, their forward passes, and training procedures are presented in the following subsections.

1) *Self-supervised Transformer*: Fig. 3 illustrates the backbone architecture of the self-supervised transformer, which serves as the long-term memory of CLAD-Net. The standard transformer architecture is typically made up of an encoder-decoder for data reconstruction. We adapt this design by retaining only the encoder and framing it as a self-supervised learning task.

Let  $\mathbf{x} \in \mathbb{R}^{l \times d}$  represent the input time-series segment, where  $d$  is the total number of sensor channels and  $l$  is the sequence (window) length. In many sensor-based HAR systems, sensors are positioned on multiple distinct body regions. To exploit this structure, we assume that the  $d$  sensor channels are grouped into  $n$  non-overlapping subsets, each associated with a specific body part. We denote this partition as  $\mathbf{x}^{(1)}, \mathbf{x}^{(2)}, \dots, \mathbf{x}^{(n)}$ , where  $\mathbf{x}^{(i)} \in \mathbb{R}^{l \times d_i}$  and  $\sum_{i=1}^n d_i = d$ . This grouping allows

the model to encode localized representations for each body region, rather than treating the input as a flat sequence of sensor channels. These body-part-specific segments are then processed independently in downstream modules.

Subsequently, each body-part segment is passed through an encoder to extract localized features. This step is analogous to Vision Transformers [42], where image patches are projected into a shared embedding space. Formally, for each body part, the encoder is a parameterized learnable function  $f_{\text{embed},i} : \mathbb{R}^{l \times d_i} \rightarrow \mathbb{R}^{l \times d_{\text{model}}}$  mapping raw sensor inputs to a fixed-dimensional latent space. The resulting embeddings are then enriched with temporal information using a fixed sinusoidal positional encoder,  $g_{\text{pos}} : \mathbb{R}^{l \times d_{\text{model}}} \rightarrow \mathbb{R}^{l \times d_{\text{model}}}$  [49]. This step allows the model to distinguish events not just by what occurred, but also by when they occurred. The encoded and temporally-aware segments are then ready to be processed by the attention mechanism that follows.

At this stage, we have  $n$  temporally encoded body-part representations denoted as  $\{\mathbf{z}^{(1)}, \dots, \mathbf{z}^{(n)}\}$ , where each  $\mathbf{z}^{(i)} = g_{\text{pos}}(f_{\text{embed},i}(\mathbf{x}^{(i)}))$  represents the embedded and positionally encoded signal from the  $i$ -th body region.

To capture interdependencies between body parts, we apply an  $n$ -branch multi-head cross-attention mechanism across these representations. Each branch computes the attention between a shared query signal  $\mathbf{z}^{(q)}$  (from a designated reference body part) and a distinct body-part representation  $\mathbf{z}^{(i)}$  used as both key and value. This setup allows the query region to selectively incorporate contextual information from other body regions.

The attention in each branch is computed using the standard scaled dot-product attention:

$$\text{Attention}(\mathbf{Q}, \mathbf{K}, \mathbf{V}) = \text{Softmax} \left( \frac{\mathbf{Q}\mathbf{K}^T}{\sqrt{d_{\text{model}}}} \right) \mathbf{V}. \quad (1)$$

For the  $i$ -th cross-attention branch with  $m_H$  heads, we compute:

$$\text{CrossAttn}(\mathbf{z}^{(q)}, \mathbf{z}^{(i)}) = \left[ \mathbf{H}_1^{(i)}, \dots, \mathbf{H}_{m_H}^{(i)} \right] \mathbf{W}_{\mathbf{H}}^{(i)}, \quad (2)$$

Where each head output is defined as:

$$\mathbf{H}_h^{(i)} = \text{Attention} \left( \mathbf{z}^{(q)} \mathbf{W}_{\mathbf{Q}_h}^{(i)}, \mathbf{z}^{(i)} \mathbf{W}_{\mathbf{K}_h}^{(i)}, \mathbf{z}^{(i)} \mathbf{W}_{\mathbf{V}_h}^{(i)} \right). \quad (3)$$

Here:

- $\mathbf{W}_{\mathbf{Q}_h}^{(i)}, \mathbf{W}_{\mathbf{K}_h}^{(i)}, \mathbf{W}_{\mathbf{V}_h}^{(i)} \in \mathbb{R}^{d_{\text{model}} \times d_{\text{model}}}$  are the learnable projection matrices for the  $h$ -th head in the  $i$ -th branch.
- $\mathbf{W}_{\mathbf{H}}^{(i)} \in \mathbb{R}^{(m_H \cdot d_{\text{model}}) \times d_{\text{model}}}$  is the output projection matrix that maps the concatenated head outputs back to the original model dimension.

This multi-branch structure enables the model to retain a fixed query representation while attending to multiple body-part signals in parallel. The outputs from all attention branches are then aggregated and forwarded to the subsequent layers of the transformer architecture.

The final stage of the transformer comprises three stacked feedforward blocks, each followed by a residual connection and layer normalization. The process begins by normalizing

the cross-attention output before passing it to the first feed-forward layer. The output of this layer is added back to its input, followed by another layer normalization and a second feedforward transformation. This pattern is repeated once more, yielding a total of three feedforward layers interleaved with Add & Norm operations.

As discussed earlier, the transformer is trained in a self-supervised manner using a contrastive objective. Although several loss functions can be employed in this framework, we adopt the Barlow Twins loss [50] following its successful application [22], [51]. To compute this loss, we generate two distinct augmentations of the input sample  $\mathbf{x}$ , denoted as  $\bar{\mathbf{x}}$  and  $\hat{\mathbf{x}}$ . These augmented views are created using time-series-specific transformations, such as additive Gaussian noise or crop and resize. We evaluate the effect of different augmentation strategies empirically in the results section. Each augmented input is passed independently through the transformer  $\Psi$ , producing the output representations  $\bar{\mathbf{r}} = \Psi(\bar{\mathbf{x}})$  and  $\hat{\mathbf{r}} = \Psi(\hat{\mathbf{x}})$ . The Barlow Twins loss is then computed by first forming a cross-correlation matrix between the batch-normalized outputs:

$$\mathbf{C}_{ij} = \frac{\sum_{b=1}^B \bar{r}_{b,i} \cdot \hat{r}_{b,j}}{\sqrt{\sum_{b=1}^B (\bar{r}_{b,i})^2} \cdot \sqrt{\sum_{b=1}^B (\hat{r}_{b,j})^2}}, \quad (4)$$

Where  $B$  is the batch size, and  $\bar{r}_{b,i}$  and  $\hat{r}_{b,j}$  refer to the  $i$ -th and  $j$ -th feature dimensions of the  $b$ -th sample from the representations  $\bar{\mathbf{r}}$  and  $\hat{\mathbf{r}}$ , respectively.

The loss function encourages the diagonal elements of  $\mathbf{C}$  to be close to 1 (maximizing agreement between the two views) while minimizing the off-diagonal terms (decorrelating features):

$$\mathcal{L}_{\text{BT}} = \sum_i (1 - \mathbf{C}_{ii})^2 + \lambda_{\text{BT}} \sum_i \sum_{i \neq j} \mathbf{C}_{ij}^2 \quad (5)$$

Where  $\lambda_{\text{BT}}$  is a hyperparameter that balances the redundancy reduction term. Algorithm 1 summarizes the forward and the training procedure of the transformer module.

2) *Supervised Convolutional Neural Network*: In parallel with the self-supervised transformer, our system includes a supervised CNN designed for the downstream task of activity classification. Unlike the transformer, which operates independently of labels and task identity, the CNN is trained in a fully supervised and task-aware setting—meaning it has access to both activity labels and the subject identifier during training. This allows the CNN to optimize directly for subject-specific decision boundaries.

The CNN architecture comprises three convolutional blocks. Each block contains four layers of 1D convolutions, followed by an average pooling layer and a nonlinearity. We add a residual connection and apply layer normalization after every block, resembling the Add & Norm structure used in transformer and ResNet architectures. The final output of the CNN is concatenated with the transformer’s final representation vector, and the combined feature is passed to a linear classifier for prediction.

We train the CNN using a knowledge distillation [52] approach inspired by Learning without Forgetting (LwF) [20].

---

**Algorithm 1** Self-Supervised Transformer Training with Barlow Twins Loss

---

**Require:** Input time-series batch  $\{\mathbf{x}_b\}_{b=1}^B$ , augmentations  $\mathcal{A}_1$ ,  $\mathcal{A}_2$ , body partitioning function  $\mathcal{P}$ , optimizer  $\mathcal{O}$

- 1: **Augment input samples:**
- 2: **for**  $b = 1$  to  $B$  **do**
- 3:    $\bar{\mathbf{x}}_b \leftarrow \mathcal{A}_1(\mathbf{x}_b)$
- 4:    $\hat{\mathbf{x}}_b \leftarrow \mathcal{A}_2(\mathbf{x}_b)$
- 5: **end for**
- 6: **Forward pass through transformer:**
- 7: **for**  $b = 1$  to  $B$  **do**
- 8:   **for**  $s \in \{\bar{\mathbf{x}}_b, \hat{\mathbf{x}}_b\}$  **do**
- 9:     Partition input into  $n$  body parts:  $\{\mathbf{x}^{(i)}\}_{i=1}^n \leftarrow \mathcal{P}(s)$
- 10:     **for**  $i = 1$  to  $n$  **do**
- 11:        $\mathbf{e}^{(i)} \leftarrow f_{\text{embed},i}(g_{\text{pos}}(\mathbf{x}^{(i)}))$
- 12:        $\mathbf{z}^{(i)} \leftarrow g_{\text{pos}}(\mathbf{e}^{(i)})$
- 13:     **end for**
- 14:     Select query part  $\mathbf{z}^{(q)}$  (e.g., hand)
- 15:     **for**  $i = 1$  to  $n$  **do**
- 16:        $\mathbf{a}^{(i)} \leftarrow \text{CrossAttn}(\mathbf{z}^{(q)}, \mathbf{z}^{(i)})$
- 17:     **end for**
- 18:      $\mathbf{a} \leftarrow \text{Aggregate}(\{\mathbf{a}^{(i)}\}_{i=1}^n)$
- 19:      $\mathbf{a} \leftarrow \text{FF}_1(\text{Norm}_1(\text{Dropout}(\mathbf{a})))$
- 20:      $\mathbf{a} \leftarrow \text{FF}_2(\text{Norm}_2(\mathbf{a} + \text{Dropout}(\mathbf{a})))$
- 21:      $\mathbf{r}_b \leftarrow \text{FF}_3(\text{Norm}_3(\mathbf{a} + \text{Dropout}(\mathbf{a})))$
- 22: **end for**
- 23: **end for**
- 24: **Compute Barlow Twins loss:**
- 25: Normalize outputs:  $\bar{\mathbf{r}}, \hat{\mathbf{r}} \in \mathbb{R}^{B \times d_{\text{model}}}$
- 26: Compute cross-correlation matrix
- 27: Compute loss  $\mathcal{L}_{\text{BT}}$
- 28: **Backward pass:**
- 29: Compute gradients:  $\nabla_{\theta} \mathcal{L}_{\text{BT}}$
- 30: Update model parameters:  $\theta \leftarrow \mathcal{O}(\theta, \nabla_{\theta} \mathcal{L}_{\text{BT}})$

---

Specifically, after training on the final batch of subject  $t - 1$ , we store a frozen copy of the model’s parameters, denoted as  $\theta_{t-1}$ . When training on the subsequent subject  $t$ , we minimize a combined loss function that balances prediction accuracy and output consistency with the previous model:

$$\mathcal{L}_{\text{total}} = \mathcal{L}_{\text{CE}}(f_{\theta_t}(\mathbf{x}), y) + \lambda_{\text{distill}} \cdot \mathcal{L}_{\text{distill}}(f_{\theta_t}(\mathbf{x}), f_{\theta_{t-1}}(\mathbf{x})) \quad (6)$$

Where  $\mathbf{x}$  and  $y$  are the input-label pairs from subject  $t$ , and  $\lambda_{\text{distill}}$  is a hyperparameter that controls the trade-off between classification accuracy and knowledge preservation. The distillation term is defined as the Kullback–Leibler (KL) divergence between the output distributions of the current model and those of the frozen model. Note that we do not store or replay any data from previous subjects. The only retained information is the snapshot of the model parameters  $\theta_{t-1}$  after training on subject  $t - 1$ . Algorithm 2 summarizes the forward process and the training procedure of the CNN module.

---

**Algorithm 2** Forward and Training Procedure of Supervised CNN with Transformer Fusion
 

---

**Require:** Input time-series segment  $\mathbf{x} \in \mathbb{R}^{l \times d}$ , transformer output  $\mathbf{r} \in \mathbb{R}^{l \times d_{\text{model}}}$ , ground truth label  $y$ , model parameters  $\theta$ , previous model parameters  $\theta_t$ , loss weight  $\lambda$ , optimizer  $\mathcal{O}$

- 1: Initialize feature tensor:  $\mathbf{h} \leftarrow \mathbf{x}$
- 2: **for**  $i = 1$  to  $3$  **do**
- 3:    $\mathbf{h}_{\text{block}} \leftarrow \text{CNNBlock}_i(\mathbf{h})$
- 4:    $\mathbf{h} \leftarrow \text{LayerNorm}(\mathbf{h} + \mathbf{h}_{\text{block}})$
- 5: **end for**
- 6: **Fuse with transformer output:**
- 7:  $\mathbf{o} \leftarrow \text{Concat}(\mathbf{h}, \mathbf{r})$
- 8: **Classification:**
- 9:  $\hat{y} \leftarrow \text{LinearClassifier}(\mathbf{o})$
- 10: **Compute Total Loss:**
- 11:  $\mathcal{L}_{\text{CE}} \leftarrow \text{CrossEntropy}(\hat{y}, y)$
- 12: **if** previous model  $f_{\theta_t}$  exists **then**
- 13:    $\mathcal{L}_{\text{distill}} \leftarrow \|f_{\theta}(x) - f_{\theta_t}(x)\|_2^2$
- 14:    $\mathcal{L}_{\text{total}} \leftarrow \mathcal{L}_{\text{CE}} + \lambda \cdot \mathcal{L}_{\text{distill}}$
- 15: **else**
- 16:    $\mathcal{L}_{\text{total}} \leftarrow \mathcal{L}_{\text{CE}}$
- 17: **end if**
- 18: **Backward pass:**
- 19: Compute gradients  $\nabla_{\theta} \mathcal{L}_{\text{total}}$
- 20: Update model parameters:  $\theta \leftarrow \mathcal{O}(\theta, \nabla_{\theta} \mathcal{L}_{\text{total}})$

---

## IV. EXPERIMENTS

In this section, we begin by introducing the datasets used to evaluate our proposed system, followed by a description of the employed evaluation metrics. We then outline the implementation details of our framework and present a series of experiments, including ablation studies, to assess the effectiveness of each component.

### A. Benchmarks

1) *PAMAP2 Physical Activity Monitoring* [10]: The dataset consists of inertial sensor recordings from 8 subjects, each performing 12 predefined activities. An additional set of 6 optional activities was included in the original dataset, but these were excluded from our analysis due to inconsistent subject participation. IMU sensors were positioned on three body regions: the dominant hand, chest, and dominant ankle. Each region was equipped with three sensor modalities—accelerometer, gyroscope, and magnetometer—resulting in a total of 9 sensor channels. All sensors were sampled at 100 Hz.

2) *Daily and Sports Activities* [53]: This dataset includes sensor recordings from 8 subjects performing 18 distinct activities. IMU sensors were installed on five body regions: the torso, left arm, right arm, left leg, and right leg. Each body part was equipped with an accelerometer, gyroscope, and magnetometer, resulting in a total of 15 sensor channels. All sensors were sampled at a frequency of 25 Hz.

### B. Evaluation Metrics

1) *Final Accuracy*: This metric quantifies the model's ability to maintain performance across all subjects after sequential training is complete and reflects how well knowledge is preserved in the final model state. Mathematically:

$$\text{FA} = \frac{1}{T} \sum_{t \in \{1, \dots, T\}} A_{t,T} \quad (7)$$

where  $A_{t,T}$  is the accuracy on subject  $t$  after training on all  $T$  subjects.

2) *Forgetting Measure*: This metric captures the severity of catastrophic forgetting. It quantifies the stability of previously acquired knowledge by measuring the decline in performance on earlier subjects. Mathematically:

$$\text{FM} = \frac{1}{T} \sum_{t \in \{1, \dots, T\}} \max_{t' \in \{1, \dots, T\}} A_{t,t'} - A_{t,T} \quad (8)$$

where  $A_{t,t'}$  is the accuracy on subject  $t$  after training on the subject  $t'$ .

3) *Learning Accuracy*: This metric evaluates the model's plasticity by measuring how effectively it acquires new knowledge when first presented with each subject. Mathematically:

$$\text{LA} = \frac{1}{T} \sum_{t \in \{1, \dots, T\}} A_{t,t} \quad (9)$$

where  $A_{t,t}$  is the accuracy on subject  $t$  immediately after training on subject  $t$ .

### C. Implementation Details

For both datasets, we applied an overlapping window segmentation approach using a window size of 2 seconds and a 50% overlap between successive windows. From each subject's segmented data, 80% was used for training and the remaining 20% for testing. To account for inter-subject variability in sensor measurements, we performed per-subject standardization by normalizing the data to zero mean and unit variance. In both benchmarks, the dominant hand was used as the query input for the cross-attention mechanism, while the key and value inputs included all body parts, including the hand.

The transformer was trained using a crop-and-resize strategy, where a continuous half of the input time-series segment was randomly cropped and then resized to its original length via interpolation. The embedding module consisted of a linear projection, followed by a sinusoidal positional encoding to inject temporal information. Each feedforward block comprised two linear layers with ReLU activation. The model was optimized using the Barlow Twins loss (with  $\lambda_{\text{BT}} = 1$ ) over 50 epochs with a learning rate of 0.001.

For the supervised CNN module, we used three stacked convolutional blocks, each containing four convolutional layers followed by average pooling and a ReLU activation. The final classification layer was a linear projection. Both the CNN and classifier were trained for 50 epochs using the Adam optimizer with a learning rate of 0.001 and incorporating a distillation loss (with  $\lambda_{\text{distill}} = 1$ ) when parameters from the previous frozen model were available.

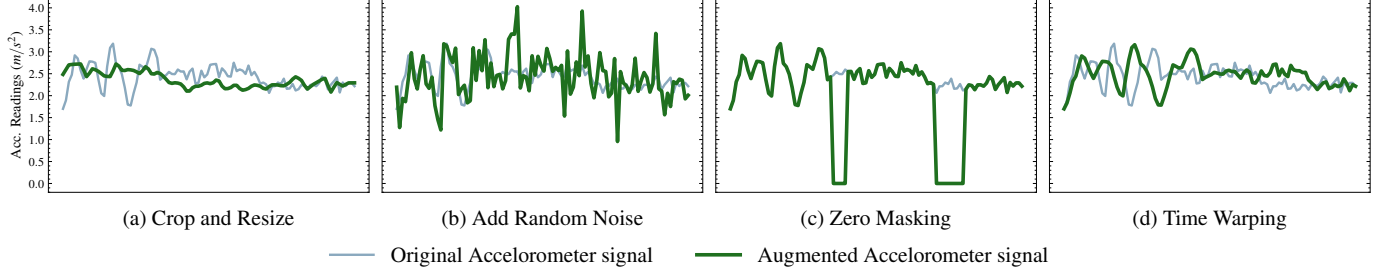


Fig. 4. Visualization of four different time-series augmentation methods applied to a sample accelerometer signal.

#### D. Results on benchmarks

We compared CLAD-Net with several common approaches in domain-incremental learning, including Learning without Forgetting (LwF) [20], Elastic Weight Consolidation (EWC) [3], and Experience Replay (ER) [15] in table I. We used the same CNN backbone in our experiments. We observed that CLAD-Net outperforms all baselines in terms of final accuracy and forgetting across both datasets. For learning accuracy, most models showed similar performance, with ER slightly ahead—possibly because it reinforces the most recent data more directly. Overall, CLAD-Net shows a better trade-off between remembering old subjects and learning from new ones.

TABLE I  
COMPARISON OF CLAD-NET WITH BASELINE DOMAIN-INCREMENTAL LEARNING METHODS ON THE PAMAP2 AND DNSA DATASETS.

Model	PAMAP2			DnSA		
	FA ↑	FM ↓	LA ↑	FA ↑	FM ↓	LA ↑
LwF	88.95	10.06	99.01	96.74	3.23	99.97
EWC	86.55	12.75	99.23	94.21	5.82	99.91
ER	88.80	10.19	<b>99.99</b>	95.92	3.42	<b>100.0</b>
CLAD-Net	<b>91.36</b>	<b>8.78</b>	99.14	<b>99.00</b>	<b>1.58</b>	99.98

To further evaluate CLAD-Net, we also compared it with ConvBoost [30], a leading ensemble-based method for activity recognition that leverages diversity techniques like mixup augmentation, channel dropout, and dynamic data sampling. We experimented with three ConvBoost variants, each using a different backbone: a standard CNN, a ConvLSTM, and an attention-based RCNN model. As shown in Table II, all three versions achieved strong learning accuracy, suggesting that ConvBoost can learn useful representations when trained on individual subjects. However, since none of these variants include explicit continual learning strategies, they suffered from notably higher forgetting rates compared to CLAD-Net. This comparison underscores that even high-performing HAR models may struggle in continual learning scenarios without mechanisms specifically designed to retain knowledge over time.

#### E. Ablation Study of CLAD-Net’s Components

We now examine the contribution of the two main aspects of CLAD-Net—specifically, the impact of the self-supervised

TABLE II  
COMPARISON OF CLAD-NET WITH CONVBOOST VARIANTS ON THE PAMAP2 AND DNSA DATASETS.

Model	PAMAP2			DnSA		
	FA ↑	FM ↓	LA ↑	FA ↑	FM ↓	LA ↑
ConvBoost (CNN)	70.70	28.52	99.22	83.72	16.10	99.99
ConvBoost (ConvLSTM)	67.57	30.74	98.82	80.26	18.63	99.88
ConvBoost (Att. Model)	82.27	17.29	<b>99.58</b>	84.94	14.69	<b>100.00</b>
CLAD-Net	<b>91.36</b>	<b>8.78</b>	99.14	<b>99.00</b>	<b>1.58</b>	99.98

transformer and the knowledge distillation mechanism. First, we remove the distillation loss and train the CNN blocks using only the classification loss. Then, we remove the transformer module while keeping the distillation loss, so the CNN is still trained with knowledge transferred from the previous subject. Finally, we disable both components, leaving just a plain CNN trained with classification loss only.

TABLE III  
ABLATION STUDY ON THE PAMAP2 AND DNSA DATASETS SHOWING THE IMPACT OF THE SELF-SUPERVISED TRANSFORMER AND THE KNOWLEDGE DISTILLATION MODULES IN CLAD-NET.

Model	PAMAP2			DnSA		
	FA ↑	FM ↓	LA ↑	FA ↑	FM ↓	LA ↑
CLAD-Net w/o Distillation	83.36	16.42	<b>99.75</b>	92.23	7.82	<b>100.0</b>
CLAD-Net w/o Transformer	88.95	10.06	99.01	96.74	3.23	99.97
CNN Baseline (No CL)	80.42	19.56	99.66	90.17	10.11	99.96
CLAD-Net	<b>91.36</b>	<b>8.78</b>	99.14	<b>99.00</b>	<b>1.58</b>	99.98

According to table III, our complete model, CLAD-Net, achieves the best performance across all setups. It’s worth noting that the final stripped-down version essentially behaves like a standard classifier without any continual learning mechanism, and it performs the worst by a noticeable margin—showing that ignoring CL in such architectures can significantly hurt performance.

#### F. Ablation Study of Self-Supervised Transformer

We now study the effect of different components within the transformer; namely, we study the effect of applying different loss functions, different augmentation methods, and different attention mechanisms.

1) *SSL Loss Functions*: We begin by evaluating the effect of different loss functions used to train the transformer. Specifically, we compare three widely adopted self-supervised learning losses: Barlow Twins [50], SimCLR [54], and BYOL [25].

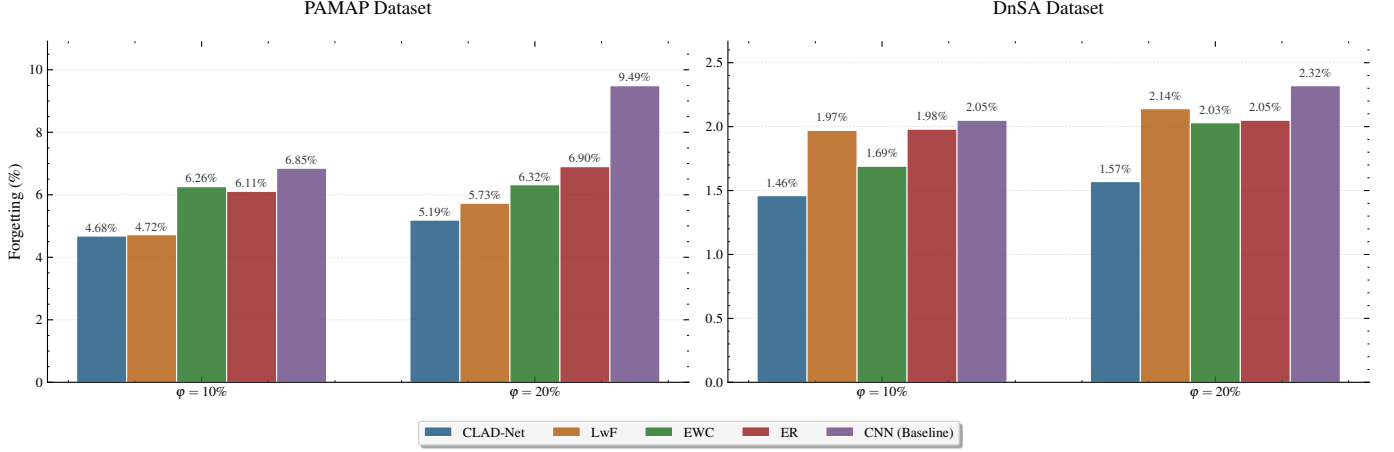


Fig. 5. Forgetting comparison across different models under 10% and 20% label availability on the PAMAP2 (left) and DnSA (right) datasets. CLAD-Net consistently shows lower forgetting than other methods.

Barlow Twins encourages the embeddings from two views to be highly correlated across matching dimensions while minimizing redundancy across different dimensions by pushing the cross-correlation matrix toward the identity. SimCLR, on the other hand, uses contrastive learning to pull together representations of positive pairs (i.e., two augmented versions of the same input) while pushing apart those of different inputs. BYOL follows a teacher-student framework, where a momentum-updated target network guides a student network to produce consistent representations from two augmented views of the same input—without relying on negative samples.

TABLE IV  
COMPARISON OF SELF-SUPERVISED LEARNING LOSS FUNCTIONS USED  
WITHIN THE TRANSFORMER MODEL.

SSL Method	PAMAP2			DnSA		
	FA $\uparrow$	FM $\downarrow$	LA $\uparrow$	FA $\uparrow$	FM $\downarrow$	LA $\uparrow$
BYOL	86.84	11.55	97.53	97.51	2.46	99.97
Contrastive	89.05	10.64	99.04	97.74	2.22	99.98
Barlow Twins	<b>91.36</b>	<b>8.78</b>	<b>99.14</b>	<b>99.00</b>	<b>1.58</b>	<b>99.98</b>

According to table IV and as previously demonstrated in works such as [55] and [22], we also observed that the Barlow Twins loss achieves superior performance across evaluation metrics. Moreover, this loss function is particularly well-suited for real-world applications due to its ability to avoid reliance on negative pairs or large batch sizes.

2) *Augmentation Methods*: Before training the self-supervised model with the Barlow Twins loss, two distinct views of the input must be generated using augmentation techniques designed for time-series data. We evaluated four such augmentation methods and selected the one that performed best for our model. Fig. 4 illustrates the effect of these four methods on a randomly chosen accelerometer time series. The corresponding performance results are summarized in Table V. As shown, the crop-and-resize method slightly outperforms the others, particularly in terms of the forgetting ratio. Based on these results, we used this augmentation method to train CLAD-Net.

TABLE V  
COMPARISON OF DIFFERENT AUGMENTATION METHODS USED WITHIN  
THE TRANSFORMER MODEL.

Augmentation Method	PAMAP2			DnSA		
	FA $\uparrow$	FM $\downarrow$	LA $\uparrow$	FA $\uparrow$	FM $\downarrow$	LA $\uparrow$
Random Noise	88.67	10.43	99.11	97.51	2.46	99.97
Zero Masking	89.32	9.74	99.04	97.54	2.42	99.98
Time Warping	89.00	10.23	99.24	97.88	2.12	99.99
<b>Crop and Resize</b>	<b>91.36</b>	<b>8.78</b>	<b>99.14</b>	<b>99.00</b>	<b>1.58</b>	<b>99.98</b>

3) *Cross-Attention vs. Self-Attention*: Finally, to demonstrate the effectiveness of cross-attention, we compared our transformer model using cross-attention blocks with an identical model that relied solely on self-attention, where each body part’s input attended only to itself. Both models were trained under the same self-supervised and continual learning setup to ensure a fair comparison. As shown in Table VI, the cross-attention model consistently outperformed its self-attention counterpart across several metrics, including classification accuracy and forgetting ratio. These results highlight that modeling inter-sensor interactions through cross-attention enhances the model’s ability to learn richer representations and better preserve knowledge across subject domains.

TABLE VI  
COMPARISON OF VARIOUS ATTENTION MECHANISMS USED WITHIN THE  
TRANSFORMER MODEL.

Attention Mechanism	PAMAP2			DnSA		
	FA $\uparrow$	FM $\downarrow$	LA $\uparrow$	FA $\uparrow$	FM $\downarrow$	LA $\uparrow$
Self Attention	87.94	11.06	99.00	97.16	2.80	99.97
<b>Cross Attention</b>	<b>91.36</b>	<b>8.78</b>	<b>99.14</b>	<b>99.00</b>	<b>1.58</b>	<b>99.98</b>

#### G. Semi-Supervised Setting

In practical scenarios, datasets are rarely fully labeled. Instead, models usually have to deal with a mix of labeled and unlabeled data. This setup often leads to lower overall accuracy, but how much a model forgets in such cases can vary quite a bit.

To explore this, we ran one last set of experiments where we randomly removed labels from most of the data, keeping only  $\varphi = 10\%$  and  $\varphi = 20\%$  of it labeled. We tested several models under these conditions. In our method, the transformer still uses all the data because its self-supervised training doesn't rely on labels. But the classifier part only sees the labeled portion during training.

Fig. 5 shows how much forgetting each method experienced under both label settings. As the figure shows, our model consistently forgets less than the others. We hypothesize that this is mostly due to the self-supervised part of CLAD-Net, especially since the LwF version—basically our model without the SSL module—performs worse in every case.

## V. CONCLUSION

In this work, we tackle the challenge of domain-incremental learning in HAR. We highlight that transferring a model trained on one subject to data from a new subject often leads to a loss in generalization due to catastrophic forgetting. This degradation stems from distributional shifts in sensor readings, as different individuals tend to perform the same activity in distinct ways. We illustrate this effect in Fig. 1, where the model's performance on earlier subjects declines as it is sequentially exposed to new ones.

To mitigate this issue, we proposed CLAD-Net, a dual-component framework designed for continual activity recognition in multi-sensor wearable settings. CLAD-Net combines a self-supervised transformer with a supervised CNN classifier, linked through knowledge distillation, to address the problem of subject-incremental learning. In Fig. 6, we apply CLAD-Net to the same sequence of subjects as in Fig. 1, showing that our model substantially reduces forgetting. Our experimental results confirm that both the self-supervised representation learner and the distillation mechanism are critical for maintaining performance across sequential tasks.

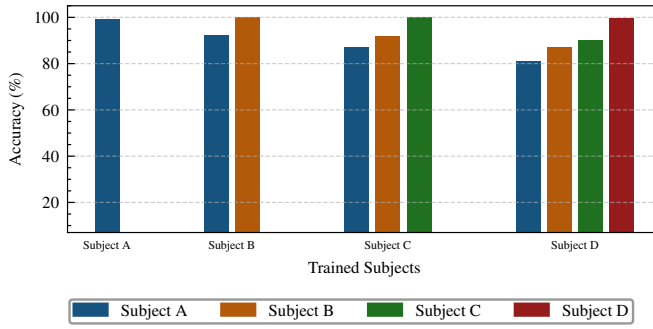


Fig. 6. CLAD-Net performance on the first four subjects from the PAMAP2 dataset.

We conducted extensive evaluations on two benchmark datasets, PAMAP2 [10] and DnSA [53], where CLAD-Net consistently outperformed baseline continual learning methods, including LwF, EWC, and ER, across metrics such as accuracy, forgetting, and learning ability. Ablation studies further demonstrated that removing either the self-supervised transformer or the knowledge distillation module leads to a noticeable drop in performance. In addition, we replaced the

cross-attention mechanism with self-attention and showed that allowing interactions across different body parts leads to better performance than having each body part attend only to itself.

For future work, we plan to extend CLAD-Net to support fully class-incremental learning settings and incorporate additional sensor modalities for more dynamic, online learning scenarios. Another important direction is to evaluate the scalability and resilience of these methods when exposed to a larger number of tasks. In particular, we are interested in understanding how the model behaves when trained on many more subjects than the limited eight available in our current datasets. Overall, our results emphasize the promise of integrating self-supervised learning, knowledge distillation, and cross-sensor attention to build more scalable and robust HAR systems.

## REFERENCES

- [1] L. Wang, X. Zhang, H. Su, and J. Zhu, “A comprehensive survey of continual learning: Theory, method and application,” 2024. [Online]. Available: <https://arxiv.org/abs/2302.00487>
- [2] R. M. French, “Catastrophic forgetting in connectionist networks,” *Trends in Cognitive Sciences*, vol. 3, no. 4, pp. 128–135, 1999. [Online]. Available: <https://www.sciencedirect.com/science/article/pii/S1364661399012942>
- [3] J. Kirkpatrick, R. Pascanu, N. Rabinowitz, J. Veness, G. Desjardins, A. A. Rusu, K. Milan, J. Quan, T. Ramalho, A. Grabska-Barwinska, D. Hassabis, C. Clopath, D. Kumaran, and R. Hadsell, “Overcoming catastrophic forgetting in neural networks,” *Proceedings of the National Academy of Sciences*, vol. 114, no. 13, p. 3521–3526, Mar. 2017. [Online]. Available: <http://dx.doi.org/10.1073/pnas.1611835114>
- [4] G. M. van de Ven and A. S. Tolias, “Three scenarios for continual learning,” 2019. [Online]. Available: <https://arxiv.org/abs/1904.07734>
- [5] J. Lu, A. Liu, F. Dong, F. Gu, J. Gama, and G. Zhang, “Learning under concept drift: A review,” *IEEE Transactions on Knowledge and Data Engineering*, p. 1–1, 2018. [Online]. Available: <http://dx.doi.org/10.1109/TKDE.2018.2876857>
- [6] P. W. Koh, S. Sagawa, H. Marklund, S. M. Xie, M. Zhang, A. Balsubramani, W. Hu, M. Yasunaga, R. L. Phillips, I. Gao, T. Lee, E. David, I. Stavness, W. Guo, B. A. Earnshaw, I. S. Haque, S. Beery, J. Leskovec, A. Kundaje, E. Pierson, S. Levine, C. Finn, and P. Liang, “Wilds: A benchmark of in-the-wild distribution shifts,” 2021. [Online]. Available: <https://arxiv.org/abs/2012.07421>
- [7] S. Meshkat Alsadat and Z. Xu, “Multi-agent reinforcement learning in non-cooperative stochastic games using large language models,” *IEEE Control Systems Letters*, vol. 8, pp. 2757–2762, 2024.
- [8] E. Soleimani and E. Nazerfard, “Cross-subject transfer learning in human activity recognition systems using generative adversarial networks,” *Neurocomputing*, vol. 426, p. 26–34, Feb. 2021. [Online]. Available: <http://dx.doi.org/10.1016/j.neucom.2020.10.056>
- [9] R. Kumar Sah, S. I. Mirzadeh, and H. Ghasemzadeh, “Continual learning for activity recognition,” in *2022 44th Annual International Conference of the IEEE Engineering in Medicine & Biology Society (EMBC)*, 2022, pp. 2416–2420.
- [10] A. Reiss, “PAMAP2 Physical Activity Monitoring,” UCI Machine Learning Repository, 2012, DOI: <https://doi.org/10.24432/C5NW2H>.
- [11] N. T. Chatrudi, W. Clegern, R. Hager, L. Nelson, and H. Ghasemzadeh, “Wavelet-augmented self-supervised learning for accurate classification of cognitive workload,” in *2024 IEEE 20th International Conference on Body Sensor Networks (BSN)*, 2024, pp. 1–4.
- [12] R. Rahimi Azghan, N. C. Glodsky, R. K. Sah, C. Cuttler, R. McLaughlin, M. J. Cleveland, and H. Ghasemzadeh, “Cudle: Learning under label scarcity to detect cannabis use in uncontrolled environments using wearables,” *IEEE Sensors Journal*, vol. 25, no. 5, pp. 9093–9100, 2025.
- [13] M. G. Sheikhlou, N. S. Ravari, M. Behrouzi, N. Goodarzi, R. S. Larijani, R. Varshochian, R. Dinarvand, and M. R. R. and, “Engineered pIgA microspheres for extended-release of naltrexone: in vitro, in vivo, and iviv,” *Pharmaceutical Development and Technology*, vol. 28, no. 2, pp. 190–199, 2023, pMID: 36688610. [Online]. Available: <https://doi.org/10.1080/10837450.2023.2172041>

[14] R. Hadsell, D. Rao, A. A. Rusu, and R. Pascanu, “Embracing change: Continual learning in deep neural networks,” *Trends in cognitive sciences*, vol. 24, no. 12, pp. 1028–1040, 2020.

[15] A. Chaudhry, M. Rohrbach, M. Elhoseiny, T. Ajanthan, P. K. Dokania, P. H. S. Torr, and M. Ranzato, “On tiny episodic memories in continual learning,” 2019. [Online]. Available: <https://arxiv.org/abs/1902.10486>

[16] L.-J. Lin, “Self-improving reactive agents based on reinforcement learning, planning and teaching,” *Machine learning*, vol. 8, pp. 293–321, 1992.

[17] Y. Liu, Y. Su, A.-A. Liu, B. Schiele, and Q. Sun, “Mnemonics training: Multi-class incremental learning without forgetting,” in *Proceedings of the IEEE/CVF conference on Computer Vision and Pattern Recognition*, 2020, pp. 12245–12254.

[18] Q. Zhang, Y. Guo, and Y. Xiang, “Continual distillation learning: Knowledge distillation in prompt-based continual learning,” 2025. [Online]. Available: <https://arxiv.org/abs/2407.13911>

[19] A. Usmanova, F. Portet, P. Lalanda, and G. Vega, “A distillation-based approach integrating continual learning and federated learning for pervasive services,” 2021. [Online]. Available: <https://arxiv.org/abs/2109.04197>

[20] Z. Li and D. Hoiem, “Learning without forgetting,” 2017. [Online]. Available: <https://arxiv.org/abs/1606.09282>

[21] J. L. McClelland, B. L. McNaughton, and R. C. O'Reilly, “Why there are complementary learning systems in the hippocampus and neocortex: insights from the successes and failures of connectionist models of learning and memory,” *Psychological review*, vol. 102, no. 3, p. 419, 1995.

[22] Q. Pham, C. Liu, and S. Hoi, “Dualnet: Continual learning, fast and slow,” 2021. [Online]. Available: <https://arxiv.org/abs/2110.00175>

[23] C. J. Tayek, L. Cherukuri, S. Hamal, and J. A. Tayek, “Importance of fasting blood glucose goals in the management of type 2 diabetes mellitus: a review of the literature and a critical appraisal,” *Journal of diabetes, metabolic disorders & control*, vol. 5, no. 4, p. 113, 2018.

[24] A. Clark, “Whatever next? predictive brains, situated agents, and the future of cognitive science,” *Behavioral and Brain Sciences*, vol. 36, no. 3, p. 181–204, 2013.

[25] J.-B. Grill, F. Strub, F. Altché, C. Tallec, P. H. Richemond, E. Buchatskaya, C. Doersch, B. Avila Pires, Z. D. Guo, M. G. Azar *et al.*, “Bootstrap your own latent: A new approach to self-supervised learning,” in *Advances in Neural Information Processing Systems (NeurIPS)*, vol. 33, 2020, pp. 21271–21284.

[26] P. Shaeri and A. Katanforoush, “A semi-supervised fake news detection using sentiment encoding and lstm with self-attention,” in *2023 13th International Conference on Computer and Knowledge Engineering (ICCKE)*, 2023, pp. 590–595.

[27] C. I. Tang, L. Qendro, D. Spathis, F. Kawsar, A. Mathur, and C. Mascolo, “Balancing continual learning and fine-tuning for human activity recognition,” 2024. [Online]. Available: <https://arxiv.org/abs/2401.02255>

[28] A. Bolatov, A. Yessenbayeva, and A. Yazici, “Glula: Linear attention-based model for efficient human activity recognition from wearable sensors,” *Wearable Technologies*, vol. 5, p. e10, 2024.

[29] A. Mamun, S. I. Mirzadeh, and H. Ghasemzadeh, “Designing deep neural networks robust to sensor failure in mobile health environments,” in *2022 44th Annual International Conference of the IEEE Engineering in Medicine & Biology Society (EMBC)*, 2022, pp. 2442–2446.

[30] S. Shao, Y. Guan, B. Zhai, P. Missier, and T. Plötz, “Convboost: Boosting convnets for sensor-based activity recognition,” *Proc. ACM Interact. Mob. Wearable Ubiquitous Technol.*, vol. 7, no. 2, Jun. 2023. [Online]. Available: <https://doi.org/10.1145/3596234>

[31] S. M. Alsadat, N. Baharisangari, Y. Paliwal, and Z. Xu, “Distributed reinforcement learning for swarm systems with reward machines,” in *2024 American Control Conference (ACC)*, 2024, pp. 33–38.

[32] S. Jha, M. Schiemer, F. Zambonelli, and J. Ye, “Continual learning in sensor-based human activity recognition: An empirical benchmark analysis,” *Information Sciences*, vol. 575, p. 1–21, Oct. 2021. [Online]. Available: <http://dx.doi.org/10.1016/j.ins.2021.04.062>

[33] M. Schiemer, L. Fang, S. Dobson, and J. Ye, “Online continual learning for human activity recognition,” *Pervasive and Mobile Computing*, vol. 93, p. 101817, 2023. [Online]. Available: <https://www.sciencedirect.com/science/article/pii/S1574119223000755>

[34] H. Yuan, S. Chan, A. P. Creagh, C. Tong, A. Acquah, D. A. Clifton, and A. Doherty, “Self-supervised learning for human activity recognition using 700,000 person-days of wearable data,” *npj Digital Medicine*, vol. 7, no. 1, Apr. 2024. [Online]. Available: <http://dx.doi.org/10.1038/s41746-024-01062-3>

[35] S.-A. Rebuffi, A. Kolesnikov, G. Sperl, and C. H. Lampert, “icarl: Incremental classifier and representation learning,” 2017. [Online]. Available: <https://arxiv.org/abs/1611.07725>

[36] G. I. Parisi, R. Kemker, J. L. Part, C. Kanan, and S. Wermter, “Continual lifelong learning with neural networks: A review,” *Neural Networks*, vol. 113, pp. 54–71, 2019. [Online]. Available: <https://www.sciencedirect.com/science/article/pii/S0893608019300231>

[37] G. M. Van de Ven, T. Tuytelaars, and A. S. Tolias, “Three types of incremental learning,” *Nature Machine Intelligence*, vol. 4, no. 12, pp. 1185–1197, 2022.

[38] E. Arani, F. Sarfraz, and B. Zonooz, “Learning fast, learning slow: A general continual learning method based on complementary learning system,” 2022. [Online]. Available: <https://arxiv.org/abs/2201.12604>

[39] A. Gomez-Villa, B. Twardowski, K. Wang, and J. van de Weijer, “Plasticity-optimized complementary networks for unsupervised continual learning,” 2023. [Online]. Available: <https://arxiv.org/abs/2309.06086>

[40] F. Szatkowski, M. Pyla, M. Przewieczkowski, S. Cygert, B. Twardowski, and T. Trzciński, “Adapt your teacher: Improving knowledge distillation for exemplar-free continual learning,” 2023. [Online]. Available: <https://arxiv.org/abs/2308.09544>

[41] S.-Y. Yin, Y. Huang, T.-Y. Chang, S.-F. Chang, and V. S. Tseng, “Continual learning with attentive recurrent neural networks for temporal data classification,” *Neural Networks*, vol. 158, pp. 171–187, 2023. [Online]. Available: <https://www.sciencedirect.com/science/article/pii/S0893608022004270>

[42] A. Dosovitskiy, L. Beyer, A. Kolesnikov, D. Weissenborn, X. Zhai, T. Unterthiner, M. Dehghani, M. Minderer, G. Heigold, S. Gelly, J. Uszkoreit, and N. Houlsby, “An image is worth 16x16 words: Transformers for image recognition at scale,” in *International Conference on Learning Representations (ICLR)*, 2021.

[43] F. Elhambakhsh, D. Grandi, and H. Ko, “A domain adaptation of large language models for classifying mechanical assembly components,” 2025. [Online]. Available: <https://arxiv.org/abs/2505.01627>

[44] C.-F. Chen, Q. Fan, and R. Panda, “Crossvit: Cross-attention multi-scale vision transformer for image classification,” 2021. [Online]. Available: <https://arxiv.org/abs/2103.14899>

[45] B. Pang, H. Zheng, and Q. Fang, “Cross-attention enhanced pyramid multi-scale network for sensor-based human activity recognition,” *IEEE Journal of Biomedical and Health Informatics*, 2024.

[46] Y. Tang, Z. Luo, and B. Wang, “Triple attention network for sensor-based human activity recognition,” *IEEE Transactions on Emerging Topics in Computational Intelligence*, vol. 6, no. 2, pp. 304–314, 2022.

[47] S. Pramanik, D. Sikdar, and S. K. Sarkar, “Transformer-based deep reverse attention network for multimodal human activity recognition,” *Engineering Applications of Artificial Intelligence*, vol. 120, p. 105869, 2023.

[48] L. Xiao, X. Zhang, Q. Li, and D. Xu, “A two-stream transformer network for sensor-based human activity recognition,” *Neurocomputing*, vol. 503, pp. 80–90, 2022.

[49] A. Vaswani, N. Shazeer, N. Parmar, J. Uszkoreit, L. Jones, A. N. Gomez, Ł. Kaiser, and I. Polosukhin, “Attention is all you need,” *Advances in neural information processing systems*, vol. 30, 2017.

[50] J. Zbontar, L. Jing, I. Misra, Y. LeCun, and S. Deny, “Barlow twins: Self-supervised learning via redundancy reduction,” in *International Conference on Machine Learning (ICML)*. PMLR, 2021, pp. 12310–12320.

[51] C. I. Tang, L. Qendro, D. Spathis, F. Kawsar, C. Mascolo, and A. Mathur, “Kaizen: Practical self-supervised continual learning with continual fine-tuning,” 2024. [Online]. Available: <https://arxiv.org/abs/2303.17235>

[52] E. Farahmand, S. B. Soumma, N. T. Chatrudi, and H. Ghasemzadeh, “Hybrid attention model using feature decomposition and knowledge distillation for glucose forecasting,” 2025. [Online]. Available: <https://arxiv.org/abs/2411.10703>

[53] B. Barshan and K. Altun, “Daily and Sports Activities.” UCI Machine Learning Repository, 2010, DOI: <https://doi.org/10.24432/CSC59F>.

[54] T. Chen, S. Kornblith, M. Norouzi, and G. Hinton, “A simple framework for contrastive learning of visual representations,” in *International Conference on Machine Learning (ICML)*. PMLR, 2020, pp. 1597–1607.

[55] E. Fini, V. G. T. da Costa, X. Alameda-Pineda, E. Ricci, K. Alahari, and J. Mairal, “Self-supervised models are continual learners,” 2022. [Online]. Available: <https://arxiv.org/abs/2112.04215>